Journal of Orthopaedic Translation 39 (2023) 21–33

Contents lists available at ScienceDirect

Journal of Orthopaedic Translation

journal homepage: www.journals.elsevier.com/journal-of-orthopaedic-translation

Netrin-1 mediates nerve innervation and angiogenesis leading to discogenic pain

Bingjie Zheng [a,e,1], Shengwen Li [b,c,1], Yufeng Xiang [a,e], Wentian Zong [a,e], Qingliang Ma [a,e], Shiyu Wang [a,e], Haihao Wu [a,e,f], Haixin Song [a,e], Hong Ren [d], Jian Chen [a,e], Junhui Liu [a,e,**], Fengdong Zhao [a,e,*]

[a] Department of Orthopaedic Surgery, Sir Run Run Shaw Hospital, Zhejiang University School of Medicine, Hangzhou, Zhejiang, 310027, China
[b] Department of Orthopedics, The Second Affiliated Hospital of Soochow University, 1055 Sanxiang Road, 215003, Suzhou, Jiangsu, China
[c] Second Department of Orthopaedics Haining People's Hospital, Jiaxing, Zhejiang, 314400, China
[d] Department of Radiology, Sir Run Run Shaw Hospital, Zhejiang University School of Medicine, Hangzhou, Zhejiang, 310027, China
[e] Key Laboratory of Musculoskeletal System Degeneration and Regeneration Translational Research of Zhejiang Province, Hangzhou, Zhejiang, 310027, China
[f] Department of Orthopedics, Hwa Mei Hospital, University of Chinese Academy of Sciences, No. 41 Northwest Street, Ningbo, Zhejiang, 315010, China

ARTICLE INFO

Keywords:
Netrin-1
Discogenic back pain
Nerve innervation
Intervertebral disc degeneration

ABSTRACT

Objective: Discogenic low back pain (LBP) is associated with nociceptive nerve fibers that grow into degenerated intervertebral discs (IVD) but the etiopathogenesis of disease is not fully understood. The purpose of this study was to clarify the role of Netrin-1 in causing discogenic LBP.

Methods: The level of nociceptive nerve innervation was examined in disc degenerative patients and rat needle-punctured models by immunohistochemistry. Nucleus pulposus (NP) cells were isolated from IVD tissues of rats and induced degeneration by interleukin-1β (IL-1β) or tumor necrosis factor α (TNFα). The candidate genes related to neuron outgrowth and migration were selected by Next-generation sequencing (NGS). CRISPR/Cas9 was used to knockdown Netrin-1 in NP cells. The impact of Netrin-1 on nerve innervation were evaluated with P2X2、NF200 staining and microfluidics assay. Meanwhile the CD31 staining and transwell assay were used to evaluate the impact of Netrin-1 in angiogenesis. The proteins and RNA extracted from NP cells related to catabolism and anabolism were examined by western blot assay and RT-qPCR experiment. ChIP and luciferase experiments were used to assess the intracellular transcriptional regulation of Netrin-1. Further, a needle-punctured rat model followed by histomorphometry and immunofluorescence histochemistry was used to explore the potential effect of Netrin-1 on LBP *in vivo*.

Results: The level of nerve innervation was increased in severe disc degenerative patients while the expression of Netrin-1 was upregulated. The supernatants of NP cells stimulated with IL-1β or TNFα containing more Netrin-1 could promote axon growth and vascular endothelial cells migration. Knocking down Netrin-1 or overexpressing transcription factor TCF3 as a negative regulator of Netrin-1 attenuated this effect. The needle-punctured rat model brought significant spinal hypersensitivity, nerve innervation and angiogenesis, nevertheless knocking down Netrin-1 effectively prevented disc degeneration-induced adverse impacts.

Conclusion: Discogenic LBP was induced by Netrin-1, which mediated nerve innervation and angiogenesis in disc degeneration. Knocking down Netrin-1 by CRISPR/Cas9 or negatively regulating Netrin1 by transcription factor TCF3 could alleviate spinal hypersensitivity.

The translational potential of this article: This study on Netrin-1 could provide a new target and theoretical basis for the prevention and treatment for discogenic back pain.

* Corresponding author. Department of Orthopaedic Surgery, Sir Run Run Shaw Hospital, Zhejiang University School of Medicine, Hangzhou, Zhejiang, 310027, China.

** Corresponding author. Department of Orthopaedic Surgery, Sir Run Run Shaw Hospital, Zhejiang University School of Medicine, Hangzhou, Zhejiang, 310027, China.

E-mail addresses: ljhzju@zju.edu.cn (J. Liu), zhaofengdong@zju.edu.cn, zhaodong68@hotmail.com (F. Zhao).

[1] These authors contributed equally to this work.

https://doi.org/10.1016/j.jot.2022.11.006
Received 29 April 2022; Received in revised form 16 September 2022; Accepted 28 November 2022

1. Introduction

Low back pain (LBP) is a worldwide disease that causes health care issues, and it is more significant than any other medical conditions [1,2], which affects people's daily life or production activities, and puts a severe financial burden on the country [3,4]. A variety of conditions can cause LBP, including disc degeneration, herniated discs, spinal stenosis, facet hypertrophy or ossification, spinal misalignment, nerve compression, and peripheral neuropathy, among which discogenic LBP is one of the most common sources of LBP [5,6].

Discogenic back pain refers to LBP caused by changes in the internal structure of the lumbar intervertebral disc (IVD) itself. It is associated with vascularized granulation tissue and nociceptive nerve fibers growing into the tissue along the radioactive fissures of the annulus fibrosus [7]. Under normal anatomical structure, the IVD is a composite tissue composed of gelatinous NP which is rich in proteoglycan and surrounded by an outer collagen-rich fibrous ring (annulus fibrosus, AF), as well as the upper and lower cartilaginous endplate (CEP) which combines the IVD. Neurons originating from the dorsal root Ganglion (DRG) innervate the outer 1/3 lamellae of the IVD annulus, and the distributed sensory nerves are mainly nociceptive neurons that expressing calcitonin gene-related peptide (CGRP) [8–11], which form the structural substrate of discogenic back pain.

During the IVD degeneration, the number of nociceptive neurons that invade IVD increase [12,13], and the invasion extends to the inner fibrous annulus and even the nucleus pulposus (NP) [7,14,15]. In addition, the inflammatory response associated with IVD degeneration exposes invaded nociceptive neurons to high levels of interleukin-6 (IL-6), tumor necrosis factor α (TNFα) and interleukin-1β (IL-1β) [16–19] and in pathologically low-pH environment [20]. TNFα, IL-1β and IL-6 have been shown to sensitize nociceptive neurons, which in turn become more sensitive to thermal and mechanical stimuli [21–23], and induce thermal hyperalgesia in peripheral neuropathy models [21,24,25], these changes promote the development of discogenic back pain. Non-surgical therapies such as pain medication, physical therapy, and exercise are usually applied in treating discogenic pain [26,27]. Nevertheless, these treatments' effectiveness is limited when it comes to severe and chronic discogenic back pain. Therefore, in-depth exploration of the mechanism of nerve and blood vessel invasion caused by IVD degeneration has important clinical significance in searching for new treatment for discogenic back pain.

Netrin-1/NTN1 is one of the Netrins family and is the first soluble axon guide factor to be discovered [28]. It is highly conserved in structure and related to laminin [29]. Netrin-1 acts as a signal that guide the growth of axons in the mammalian nervous system. It plays an important role in guiding axons and cell migration during embryonic development. Netrin-1 plays a bidirectional role in guiding axon attraction and repulsion mediated by two types of receptors: deleted in colorectal cancer (DCC) and uncoordinated 5 (UNC-5) [30–32]. Recent studies have shown that Netrin-1 is secreted by subchondral bone osteoclasts and plays an important role in osteoarthritis pain [13]. In other paper indicates that Netrin-1 secreted by osteoclasts in EP, mediating nerve invasion and causing spinal hypersensitivity pain [33]. However, these studies regard Netrin-1 as product of osteoclasts and ignore the other source. In addition, Netrin-1 can also mediate the migration of vascular endothelial cells and has a pro-angiogenic effect [30,34]. All of these results suggest that Netrin-1 may have a key role in the pathological model of discogenic back pain.

In this research, we clarified Netrin-1 plays an important role in discogenic back pain. We put forward the following research hypothesis that Netrin-1 induces nerve invasion in degenerative IVDs and promotes blood vessel growth to cause discogenic back pain. The research of this subject is of great significance to clarify the molecular mechanism of discogenic back pain, and will also provide a new target and theoretical basis for the prevention and treatment for discogenic back pain.

2. Materials and methods

2.1. Rat nucleus pulposus cells preparation and in vitro induced degeneration

Gel-like NP tissues derived from 8-week-old male Sprague–Dawley rats were digested for 2 h with 0.2% type II collagenase (Sigma, St. Louis, MO, United States). Under a 5% CO2, 37 °C environment, cells were grown in complete culture media (DMEM/F12, Gibco, Invitrogen, United States) with 10% fetal bovine serum (FBS, Gibco, Invitrogen, United States) and 1% penicillin/streptomycin. Every 2–3 days, the medium was changed until a 90% confluence was attained. Then, in triplicate, NP cells were seeded into a 12-well plate and treated with IL-1β (10 ng/ml) or TNFα (50 ng/ml) for 48 h to induce degeneration [35,36].

2.2. Immunohistochemistry and histological analysis

Human IVD specimens were obtained from the Sir Run Shaw Hospital, Zhejiang University School of Medicine. This study was approved by Research Ethics Committee of Zhejiang University. Written informed consent was obtained from all patients or their family members. The characteristics of the patients were summarized in Supplementary Table 1. The sections of human IVD specimens were used for immunohistochemical staining. 3% H_2O_2 was used to block endogenous peroxidase activity for 10 min followed by trypsin for 20 min and 5% bovine serum albumin (BSA) for 30 min to inhibit unspecific antigens. Then antibodies against P2X2, NF200 and Netrin-1 were used to incubate overnight at 4 °C. The next day, the sections were washed in PBS with 1% Tween and incubated for 1 h at room temperature with corresponding HRP-conjugated secondary antibodies (Cell Signal Technology, 1:5000). Diaminobenzidine (DAB) was used to observe the immunolabeling, which was then counterstained with hematoxylin. Three randomly-chosen fields of the NP area were used to measure the ratio of positively stained cells to total cells. Each specimen had at least three sections used, and the data were averaged. A histological grading was applied to determine the cellular and morphological changes in both the AF and NP [37]. The histological sections were assessed by three independent and blinded investigators.

2.3. RNA isolation and RT-PCR assay

NP cells obtained as above were seeded and cultured in 12-well plates with DMEM/F12 containing 10% FBS. After the induction of degeneration with IL-1β (10 ng/ml) or TNFα (50 ng/ml), total RNAs were then extracted by TRIzol reagent (Invitrogen, Carlsbad, CA, USA). 1 μg of RNAs from each sample were utilized to synthesize complementary DNA (Takara, Shiga, Japan). An ABI Prism 7500 system (Applied Biosystems, Foster City, CA, USA) with SYBR Green QPCR Master Mix (TakaraBio) were used to perform RT-qPCR experiments. The RT-qPCR system consisted of 5 μL SYBR Green QPCR Master Mix, 3 μL double-distilled water (ddH_2O), 1 μL cDNA and 10 μM each of forward and reverse primers. Target genes included Netrin-1, Collagen 2 (Col2), Sry related HMG box 9 (SOX9), A disintegrin and metalloproteinase with thrombospondin motifs 5 (ADAMTS5), Matrix metalloproteinase 13 (MMP13). The primer sequences used are shown in Supplementary Table 2. The cycle threshold (CT) data were gathered and adjusted to GAPDH, a housekeeping gene. The relative CT was determined using the $2^{-\triangle\triangle CT}$ method.

2.4. Western blot assay

The NP cells obtained as above were lysed in RIPA lysis buffer with 100 mM PMSF and phosphatase inhibitor, then centrifuged for 15 min at 12,000 rpm. Isolated supernatants were dissolved in 1 × loading buffer. The protein samples were separated by 10% SDS-PAGE gels through electroblotting and then transferred to polyvinyledene fluoride (PVDF) membranes. The membranes were then blocked for 1 h with 5% skim

milk dissolved in TBST buffer. Then PVDF membranes were divided to different protein molecular weights and incubated overnight with primary antibodies for Netrin-1, Col2, SOX9, ADAMTS5, MMP13, GAPDH and β-actin purchased from Abcam (Cambridge, MA, USA, 1:1000). The membranes were then treated for 1 h at room temperature with secondary HRP-conjugated IgG (Cell Signal Technology, 1:5000), and the protein bands were visualized using enhanced chemiluminescence reagents (Amersham Biosciences, Buckinghamshire, United States) and the LAS-4000 Science Imaging System (Fujiflm, Tokyo, Japan). The photos were analyzed using Image J software.

2.5. Enzyme-linked immunosorbent assay (ELISA)

NP cells were induced degeneration by IL-1β (10 ng/ml) or TNFα (50 ng/ml) for 48 h, after that, the original culture medium was discarded, and followed by three times washed in PBS, then replaced with fresh medium. After 72 h, the supernatants were harvested, and Netrin-1 concentrations were measured using an ELISA kit from R&D Systems (Minneapolis, MN).

2.6. CRISPR/Cas9 plasmid generation

The CRISPR/cas9 plasmid was constructed in accordance with online instructions (http://www.genome-engineering.org/crispr/). In brief, bioinformatics tools were used to select guide RNAs (gRNA) targeted at exons of NTN1 as summarized in Supplementary Table 3. We phosphorylated and self-annealed each pair of complementary oligonucleotides of gRNA for proper ligation with T4 polynucleotide kinase and T4 ligation buffer and ligated them in purified CRIPSPR/Cas9 vector pSpCas9(BB)-2 A-GFP according to the manufacturer's instructions.

2.7. Needle puncture-induced disc degeneration model and adeno-associated virus (AAV)-mediated knockdown in vivo

All animal studies in this study followed the principles and methods outlined in the National Institutes of Health (NIH) Guide for the Care and Use of Laboratory Animals, as well as the Sir Run Shaw Hospital's animal treatment standards (No. 21709. Zhejiang University affiliated, Hangzhou, Zhejiang).

A disc degeneration model and suitable controls were established using 12 male Sprague–Dawley rats for each group (about 200 g). Rats were randomly divided into sham group (no disc puncture), AAV-Null group (disc puncture, injection with AAV vector) and AAV-NTN1 gRNA group (disc puncture, injection with AAV of NTN1 CRISPR/Cas9 plasmid generated as above). The adeno-associated virus was purchased from HanHeng Biology Company (Shanghai, China).

In a brief, rats were given 0.9% (w/v) pentobarbital sodium intraperitoneally (45 mg/kg). In the AAV-Null and AAV-NTN1 gRNA group, the muscles were blunt dissected from posterior midline. And we exposed the L4/5 disc from right-side, then injected AAV vector or AAV of NTN1 CRISPR/Cas9 plasmids into L4/5 ($2.0 * 10^{12}$ vg/ml AAV titer; 2 μL injection volume was used). The needle used for AAV injection was 31G, length 8 mm (5/16″) insulin syringe needle (BD Biosciences) which has previously been shown to be safe enough to deliver materials to the NP tissue [37–39]. The drilling holes were sealed with bone wax immediately after injection. After injection, rats were left to recover for 1 week. After that, rats were punctured with a 21G needle [37,40]. In the sham group, rats were only expose the L4/5 disc from right-side.

2.8. Animal behavioral assessment

Behavioral assessment was carried out prior to surgery and every two weeks afterward. The same investigator who was blinded to the research groups conducted all behavioral assessments to prevent assessment bias.

As previously described, we used von Frey filaments to evaluate the mechanical sensitivity of the hindpaw with up-and-down method [41,42]. Briefly, rats were initially acclimatized for 1 h in individual boxes. Thereafter, a series of von Frey filaments (Aesthesio Precision Tactile Sensory Evaluator; DanMic Global LLC), initially with 2.0 g, ranging with 0.4 g, 0.6 g, 1.0 g, 1.4 g, 2 g, 4 g, 8 g, 15 g were applied. A distinct paw withdrawal or shaking was considered a positive reaction. If the reaction was positive, the following lower filament was applied, and if the reaction was negative, the following higher filament was applied. The test including 6 individual stimuli, and the reaction pattern was examined using log transforms of the von Frey force [41,43] and averaged.

Spontaneous guarding behavior was scored as: 0 - no guarding, 1 - mild shift of weight away from paw; 2 - unequal weight bearing with some part of foot not touching the floor; 3 - paw licking, foot completely raised [44]. The scores were obtained 6 observations total before von Frey filament tests and averaged.

2.9. Immunofluorescence

Rats were anesthetized with isoflurane and IVD tissue from T12 to L6 were removed and fixed in 4% paraformaldehyde for 48 h. The fixed specimens were decalcification and dehydration, and preparation of slides. The slides were treated by trypsin for 20 min and 5% PBS/BSA for 30 min to inhibit unspecific antigens, followed by permeabilized for 10min with 0.1% Triton X-100. After 1 h of blocking with 1% PBS/BSA, slides were incubated with primary antibodies against CGRP (Cell Signaling Technology, 1:200) and CD31 (abclonal, 1:200) in PBS/BSA at 4 °C overnight. Afterwards secondary antibodies conjugated with Alexa Fluor 488 and/or 594 were used to incubate cells for 1 h at room temperature. The nucleus was labelled with 10 μg/mL DAPI solution. Pictures were taken with immunofluorescence microscope (BX51TRF; Olympus, Tokyo, Japan), and the images was analyzed using Image J software.

2.10. Microfluidics assay

According to the manufacturer's instructions, Standard Neuron Device (450 μm microgroove barrier, SND450) were positioned on a cell climbing slice coated with 100 μg/mL Poly-D-Lysine (PDL, Sigma–Aldrich) overnight at 37 °C. Then the device was rinsed in sterilized ddH_2O three times before use, and DRG neurons were seeded in device at a density of 9×10^4 cells on the left side. The device was incubated at incubator for 12 h to make sure neurons were migrating into main channel of device and adhered. Each left well added 150 μL of NeuralBasal media containing 0.5 × B27 and N2 (Invitrogen, Life Technologies, Inc.) and each right well added 150 μL conditioned media. The conditioned media were 1:1 ratio of supernatants described before and NeuralBasal media. After incubated for 4 days, the DRG neurons and their nerve fibers at device were stained with conventional immunofluorescence and obtained fluorescence photographs with immunofluorescence microscope. ImageJ software was used to measure the length of nerve fibers that passed the microchannels.

2.11. Luciferase reporter assay

Briefly, HEK-293 T cells were transfected with Netrin-1 promoter luciferase plasmid with renilla (Promega). Meanwhile cells were co-transfected with vector or a particular transcription factor TCF3 (OriGene) overexpression plasmid. The dual luciferase reporter assay kit was used to evaluate luciferase activity (Beyotime, Shanghai, China). The ratio of firefly/Renilla luciferase activity was used to evaluate transcriptional activity.

2.12. Chromatin immunoprecipitation (ChIP)

NP cells were cultured with or without induction of TNFα (50 ng/ml) at 10-cm dish. After incubation for 48 h, cells were fixed in 37% formaldehyde for 10 min at room temperature. The ChIP assay was carried out

according to manufacturer's instructions of ChIP assay kit (Cell Signaling Technology). The immunoprecipitated DNA segments were collected for PCR amplification and Supplementary Table 4 shows the sequences of the oligos used in ChIP assay.

2.13. Statistical analysis

The data was provided as mean ± standard deviation (SD). Prism 8 was used to examine the data (GraphPad Software, Inc., San Diego, CA, USA). Student's t test or one-way ANOVA followed by Tukey's post hoc analysis were used to determine statistical significance, and values of $p < 0.05$ were regarded statistically significant.

3. Results

3.1. Nerve innervation in severe degenerative intervertebral disc tissue was increased

We first collected the NP specimens of IVD degeneration in clinical patients (Supplementary Table 1), and detected the invasion of nociceptive nerves in tissues by nociceptive neuron marker (P2X2) immunohistochemical staining. The percentage of positive cells in degenerative discs was higher than that in mild group (Fig. 1a and b). We also investigated the variation of nerve innervation in normal and degenerative disc in mice by needle puncture. As shown in Fig. 1c and d, at 2 weeks or 4 weeks after needle puncture, the IVD showed obvious degeneration. The immunohistochemical assays showed much more $P2X2^{+}$ and $NF200^{+}$ on junctional zone area of endplate and NP or deeper into NP tissues of needle puncture model compared with sham-operated group (Fig. 1c). The observation above primarily demonstrated that the level of nerve innervation increased associated with grade of disc degeneration.

3.2. The expression level of Netrin-1 was increased after inducing intervertebral disc degeneration

To evaluate how disc degeneration increased the level of nerve innervation, we next assessed the genes expression level of cultured NP cells treated by IL-1β (10 ng/ml) or TNFα (50 ng/ml), quantified by RNA sequencing and subjected to gene set enrichment analysis (GSEA) for pathway enrichment analysis. We focused on pathway most correlated with neural outgrowth and migration. As shown in Fig. 2a and b, the neuron migration pathway (GO: 0001764) was significantly enriched ($P = 0.045$ in IL-1β set, $P = 0.020$ in TNFα set). Contributing genes in this pathway were all upregulated (Fig. 2c and d), among which, Netrin-1 was further taken into consideration as selected by the most significant P value combined with the highest fold change for differential expression in both data sets (Fig. 2e–g, Supplementary Fig. 1). Relative mRNA expression (Fig. 2h) and protein expression of Netrin-1 increased after inducing NP cells degeneration (Fig. 2i and j). Moreover, human IVD specimens exhibited strong expression of Netrin-1 in severe degenerative discs compared with mild group (Fig. 2k and l). Taken together, these data indicated that neuron migration pathway was significantly enriched in degenerative NP cells and Netrin-1 expression level rose significantly on cellular and tissue level in disc degeneration, which might play an important role in inducing nerve innervation.

3.3. Netrin-1 attracts neural axon outgrowth and induces migration of vascular endothelia cells in vitro

To further investigate whether Netrin-1 exhibits convinced potentially causal factors for discogenic back pain, we first constructed Netrin-1 knockdown cell line by CRISPR/Cas9 (Fig. 3a and b), which showed no impact on NP cells' anabolism and catabolism (Supplementary Fig. 2a). The sequences of gRNA are shown in Supplementary Table 3. We cultured NP cells and induced degeneration by IL-1β or TNFα for 48 h, then after 3 days, the cell culture supernatant was collected as conditioned media (Fig. 3c and d). Furthermore, we examined whether Netrin-1 can regulate neuronal migration and outgrowth. For this purpose, we applied a microfluidic assay device which was used extensively in investigating axons separately from cell bodies in studies of axonal injury and regeneration *in vitro* [45]. The conditioned media exerted a clear attractive effect on neural axon compared to control cases (Fig. 3e, Supplementary Fig. 2b). Not unexpectedly, the attractive effect described above was significantly attenuated when Netrin-1 was knockdown (Fig. 3e and f, Supplementary Fig. 2c and d). These results suggested that Netrin-1 plays a potent role in promoting nerve innervation progression. In addition, variety of researches reported that ingrowth of nerve fibers was usually accompanied with neovascularization in degenerative discs, providing nutrition to the accompanying axons, which is also speculated to contribute to LBP [7,46,47]. To assess the impact of degenerative disc on angiogenic activities of endothelial cells, we used transwell migration assay with conditioned media, which showed apparent appealing effect on human umbilical vein endothelial cells (HUVECs). Whereas the silencing of Netrin-1 abrogated this effect compared to HUVECs exposed to conditioned media of degenerative NP cells (Fig. 3g and h). Collectively, we could safely draw a conclusion that degenerative NP cells mediated axonal attraction as well as the migration of vascular endothelial cells partially through extracellular level of Netrin-1.

3.4. CRISPR-mediated knockdown of Netrin-1 relieves low back pain in disc degeneration rat

With a demonstration of the appealing effect of Netrin-1 on neural axon and vascular endothelial cells *in vitro*, we took a step forward to investigate the potential effect by deletion of Netrin-1 in the needle-punctured disc degeneration rat model. Rats were injected directly into IVD of L4/5 with either AAV vector as control or AAV-NTN1 gRNA, 1 week after that, a classic disc degeneration model in L4/5 induced by needle puncture was adopted. Notably, while the model was established successfully confirmed by MRI images showing in Fig. 4a, the degree of disc degeneration showed no significantly difference between AAV-Null and AAV-NTN1 gRNA groups, which was consistent with our findings *in vitro* mentioned above (Supplementary Fig. 2a). To evaluate spinal hyperalgesia of these groups, we performed pain behavior tests, including spontaneous guarding behavior and von Frey test. Guarding behavior is regarded to be an indication of non-evoked, spontaneous pain [44], which defined as 0 (no guarding, paw flat on floor), 1 (moderate shift of weight away from paw), 2 (uneven weight bearing and some portion of the foot not contacting the floor), or 3 (foot is completely elevated or not carrying any weight). We found that although guarding behavior in both AAV-Null and AAV-NTN1 gRNA groups increased after 4 weeks, it was unique to the AAV-Null group compared to the sham group, and there was no significant difference between AAV-NTN1 gRNA and sham groups (Fig. 4b). As shown in Fig. 4c, needle punctured animals developed mechanical allodynia, as evidenced by a considerable reduction in von Frey threshold in the ipsilateral hindpaw after 4 weeks. Remarkably, we observed the threshold was significantly preserved in AAV-NTN1 gRNA group after 4 weeks, which however, also developed significant mechanical allodynia after 6 weeks compared to the sham group (Fig. 4c).

To rule out the notion that the indiscriminate effects of surgery were to blame for the mechanical hypersensitivity, we performed von Frey test on the contralateral side. Interestingly, there was also a decrease in the threshold mostly at 8 weeks, although not as significant as the reduction in the ipsilateral side (Fig. 4d). The significant increasement of CGRP targeted at or around the IVD, a hallmark of peptidergic nociceptive C nerve fibers, began at 4 weeks and till 8 weeks after needle puncture surgery with AAV vector injected according to immunofluorescent labeling. But there were no detectable or little observed CGRP+neurons around the IVD of sham-operated and AAV-NTN1 gRNA injected rats (Fig. 4e and f). Impressively, the nociceptive nerve fibers were localized

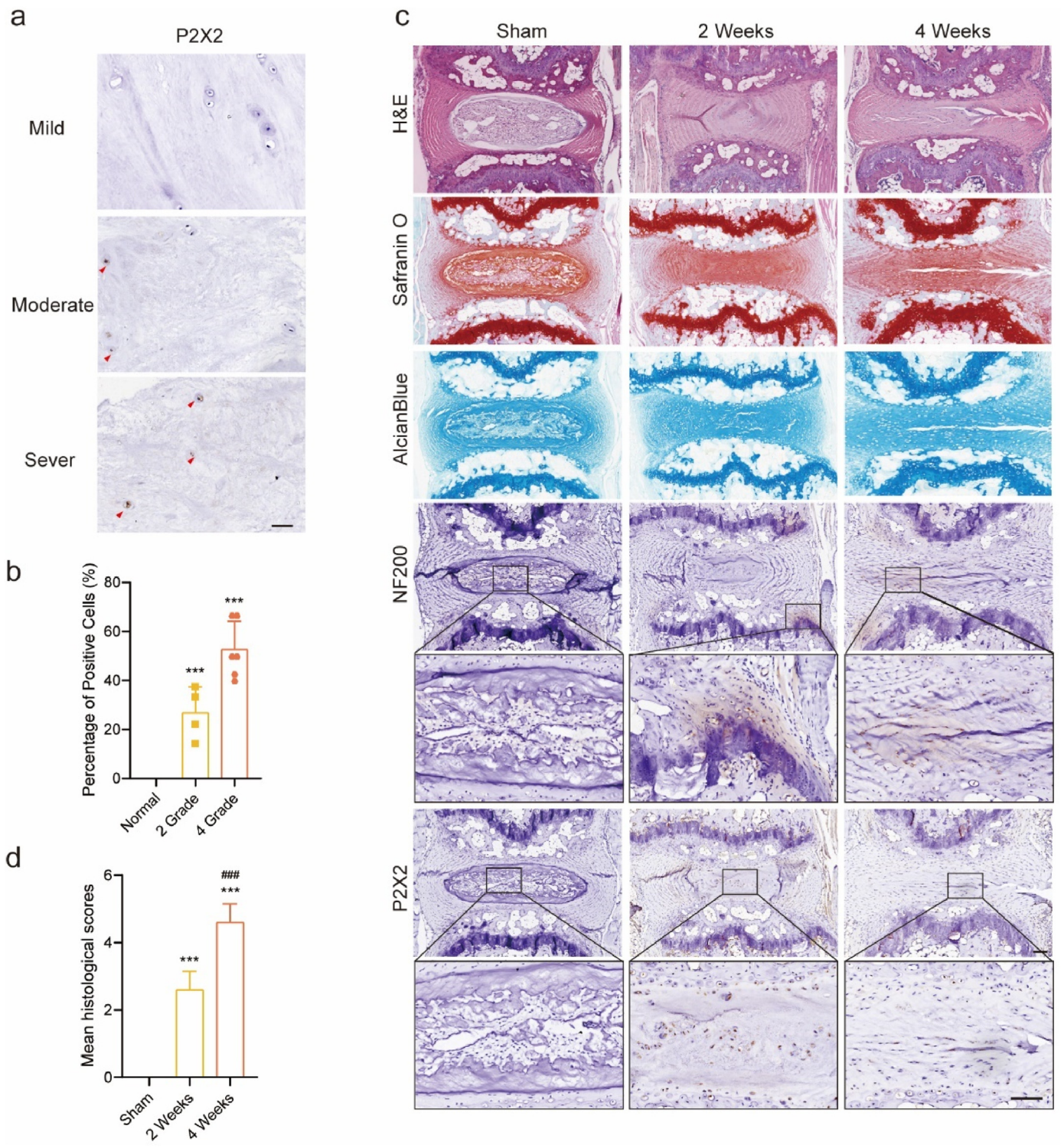

Figure 1. Nerve innervation in degenerative intervertebral disc tissue. a Immunohistochemistry to detect P2X2^{+} cells in mild, moderate and sever degenerative IVD tissues. Scale bar, 20 μm **b** Percentage of P2X2^{+} cells in IVD (n = 6, N = 2–4, each group). **p < 0.01 compared with mild group. **c** Representative images of Safranin O (second row), AlcianBlue (third row), NF200 staining (fourth row) and P2X2 staining (sixth row) of needle-punctured IVD after 2 weeks and 4 weeks. Scale bar, 80 μm **d** Histological grading scores at different time points after needle puncture. ***p < 0.001 compared with sham group, ###p < 0.001 compared with 2-week time point. Results are shown as means ± SD.

primarily adjacent to the CEP surface or outer annulus fibrosus at 4 weeks, and not invaded into the NP and inner annulus fibrosus until the discs severely degenerative at 8 weeks.

Previous studies have shown that nerves entering were co-localised with blood vessels [14]. We further investigated whether blood vessels distribution have the same characteristic with nerve fibers.

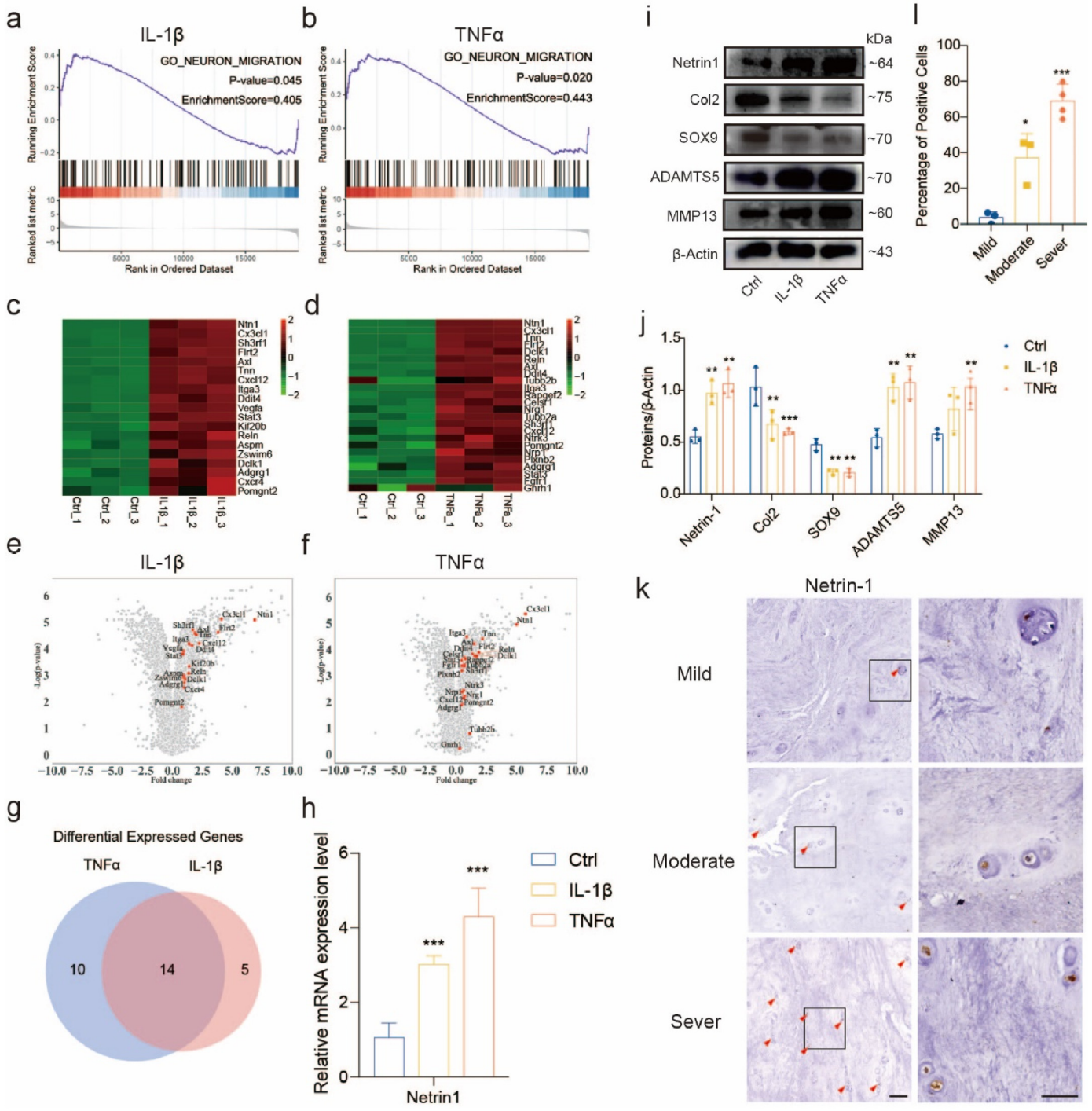

Figure 2. Netrin-1 expression level increases after inducing intervertebral disc degeneration. a Gene set enrichment analysis (GSEA) for GO_Neuron_Migration pathway enrichment analysis of cultured rat nucleus pulposus cells treated with IL-1β (10 ng/ml) or **b** TNFα (50 ng/ml) for 48 h. **c, d** Heatmaps of differential genes in GSEA set. **e, f** Volcano plots (Fold change versus P value). **g** A Venn diagram showing the intersection of differential gene sets of IL-1β (red circle) and TNFα (bule circle) groups. **h** qPCR analysis for representative differential genes Netrin-1 of degenerative nucleus pulposus cells (n = 6, each group). **i** Immunoblots showing Netrin-1 and Col2, ADAMTS5, SOX9, MMP13 in nucleus pulposus cells treated with IL-1β or TNFα for 48 h. **j** Quantification of the blot (n = 3, each group). **k** Representative immunohistochemistry of Netrin-1 in human IVD tissues. Scale bar, 80 μm (left column), 40 μm (right column). **l** Summarized analysis of percentage of positive staining (red arrow) cells (n = 4, each group). Results are shown as means ± SD. *p < 0.05, **p < 0.01, ***p < 0.001. (For interpretation of the references to colour in this figure legend, the reader is referred to the Web version of this article.)

Unexpectedly, blood vessels did not invade deep into IVD as nerve fibers, but grew toward the degenerative disc and Netrin-1 deficiency suppressed this tropism (Fig. 4g and h). Taken together, these results potently corroborated that knockdown of Netrin-1 interfered nerve innervation and blood vessels ingression, which therefore leaded to discogenic back pain *in vivo*.

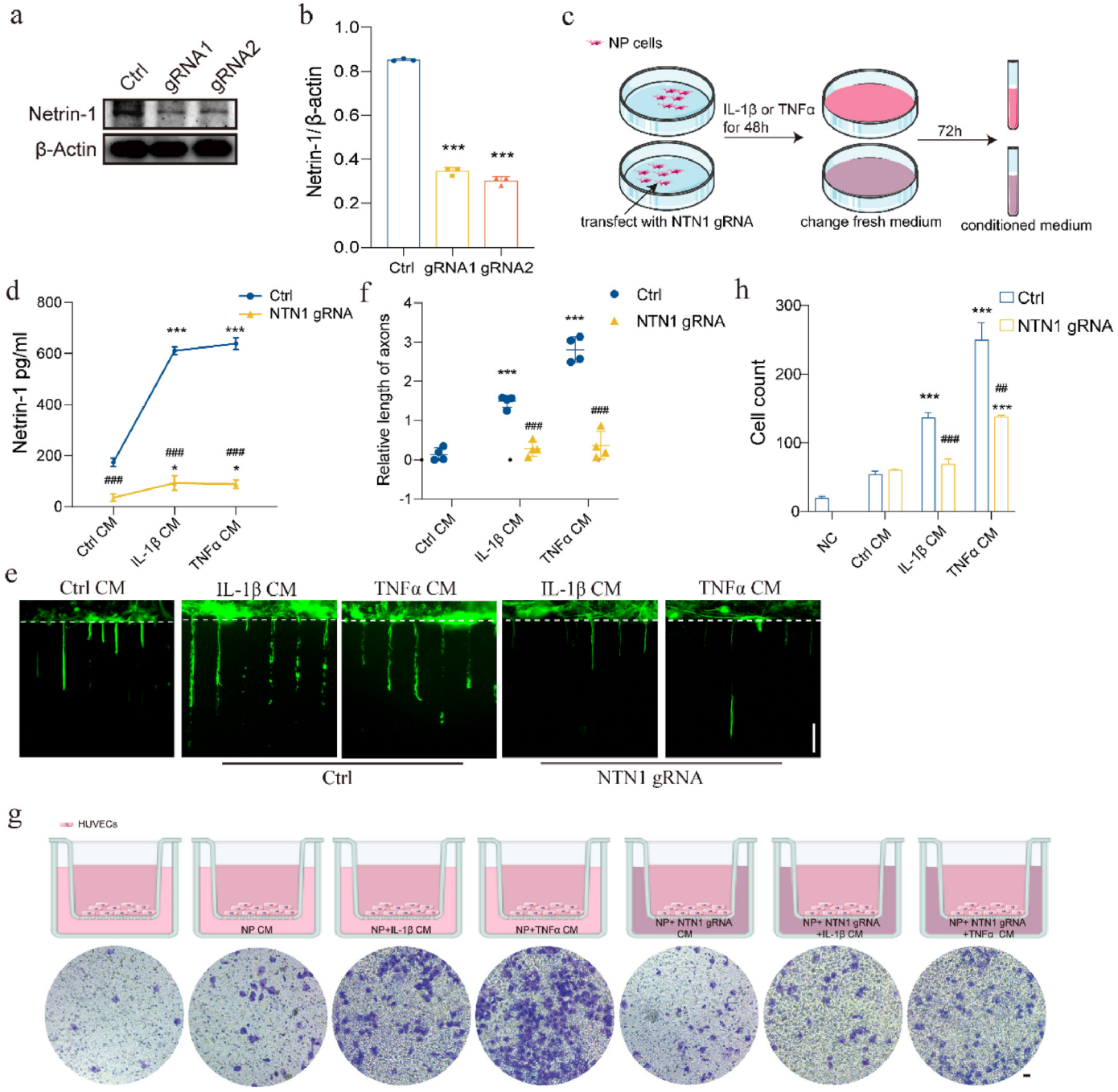

Figure 3. Netrin-1 induces axonal growth and vascular endothelia cells' migration. a The protein expression levels of Netrin-1 in Western blot of nucleus pulposus cells transfected with CRISPR/Cas9-ctrl gRNA or NTN1 gRNA1 and NTN1 gRNA2. **b** Quantification of the blot (n = 3). **c** Schematic drawing of the design for the conditioned medium (CM) model. **d** Expression of Netrin-1 in the conditioned mediums of groups as detected by ELISA (n = 5). **e** Representative photomicrographs of DRG neuron axonal outgrowth in microfluidics assay treated with nucleus pulposus cells transfected with CRISPR/Cas9-ctrl gRNA or NTN1 gRNA conditioned medium induced by IL-1β or TNFα for 48 h (n = 4). Scale bar, 100 μm **f** Analysis of the relative length of axons. **g** Transwell migration assay of human umbilical cord endothelial cells (HUVECs) co-cultured with nucleus pulposus cells transfected with CRISPR/Cas9-ctrl gRNA or NTN1 gRNA for 14 h (n = 4). Scale bar, 1 mm **h** Quantified results of mean migrate cells. Results are shown as means ± SD. *p < 0.05, **p < 0.01, ***p < 0.001 compared with ctrl groups, #p < 0.05, ##p < 0.01 ###p < 0.001 compared with groups transfected with CRISPR/Cas9-ctrl gRNA.

3.5. Retrograde and anterograde tracing of nerves found within IVDs

To figure out the source of the nerve fibers invaded into degenerative IVD, we performed a retrograde tracing experiment at 8 weeks. The neuron tracer Dil was injected into the L4/5 discs through right-sided approach which was induced degeneration before (Fig. 5a). 1 week after that, to quantify the number of Dil^+ neurons, we harvested T12 - L6 DRGs on both sides. A significant Dil^+ area was detected particularly in the right L1 and L2 DRGs, but less Dil^+ area was found in the T13 - L3 DRGs of AAV-NTN1 gRNA group though without significance (Fig. 5b and c).

To further validate the nerve innervation within L4/5 IVD derived from L1 and L2 DRGs, we carried out the anterograde tracing experiment by injecting Dil into the L1 and L2 DRGs on right sides at 8 weeks after

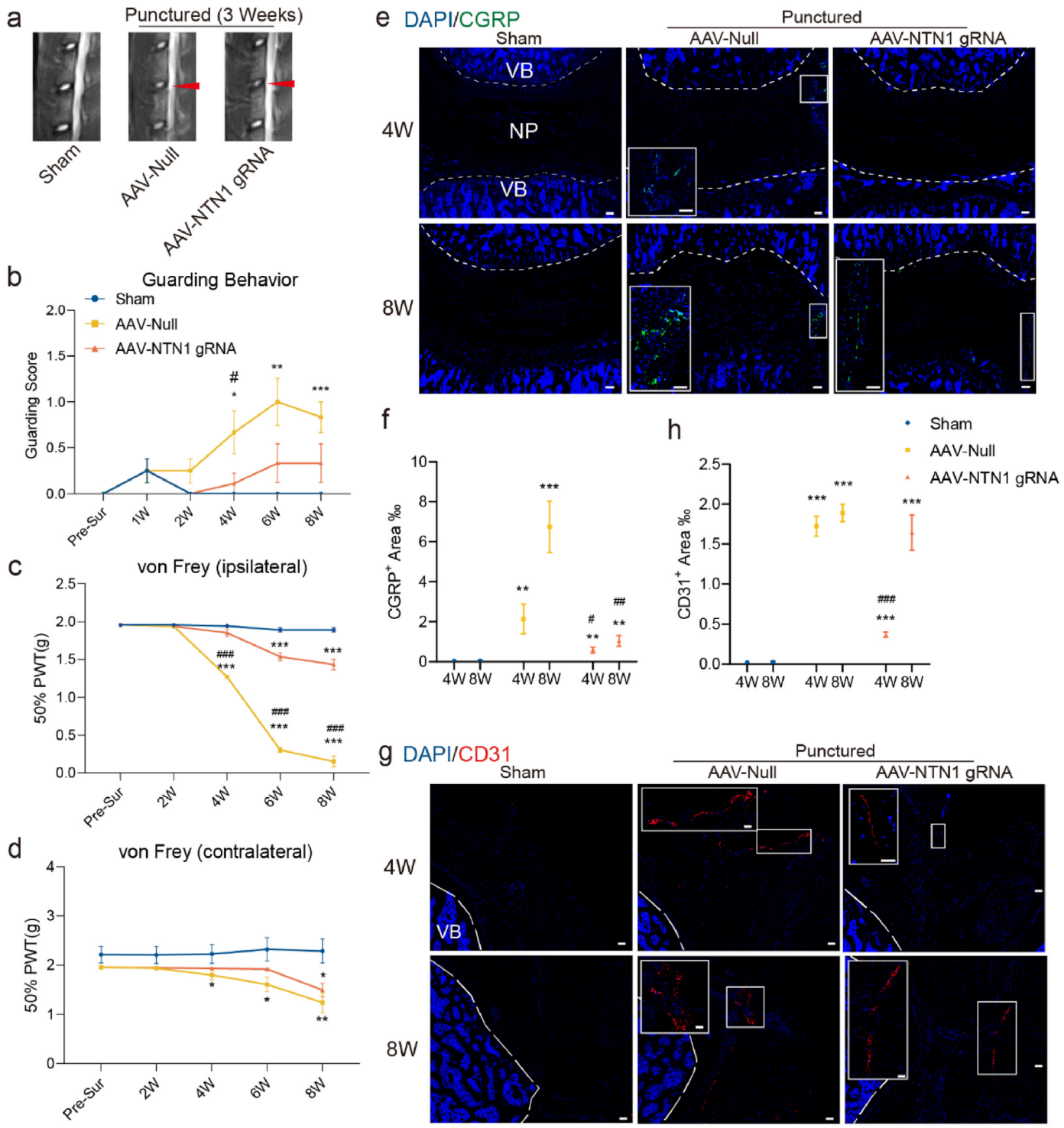

Figure 4. Animal spinal hypersensitivity pain behavior in needle-punctured rats. a Representative MRI images of L4/5 needle-punctured rats after 3 weeks **b** Analysis of guarding behavior (n = 8). Score scale: 0 - no guarding, 1 - mild shift of weight away from paw; 2 - unequal weight bearing with some part of foot not touching the floor; 3 - paw licking, foot completely raised. **c** 50% paw withdrawal threshold (PWT) of sham, AAV-Null and AAV-NTN1 gRNA groups in the ipsilateral and **d** contralateral right paws tested by von Frey filament. Results are shown as means ± SD (n = 8, each group). *p < 0.05, **p < 0.01, ***p < 0.001 compared with sham group, #p < 0.05, ##p < 0.01 ###p < 0.001 compared with AAV-Null group at the corresponding time points. **e** Representative images of immunofluorescence showing DAPI (blue), CGRP (green) of sham and needle-punctured rats transfected with AAV-Null or AAV-NTN1 gRNA at 4 weeks and 8 weeks (n = 8). Scale bar, 60 μm **f** Quantification of the CGRP $^{+}$ area. **g** Representative images of immunofluorescence showing CD31 (red) and **h** quantification of CD31^{+} area of sham and needle-punctured rats transfected with AAV-Null or AAV-NTN1 gRNA at 4 weeks and 8 weeks (n = 8). Scale bar, 60 μm. Results are shown as means ± SD (n = 8, each group). *p < 0.05, **p < 0.01, ***p < 0.001 compared with sham group, #p < 0.05, ##p < 0.01 ###p < 0.001 compared with AAV-Null group at the corresponding time points. (For interpretation of the references to colour in this figure legend, the reader is referred to the Web version of this article.)

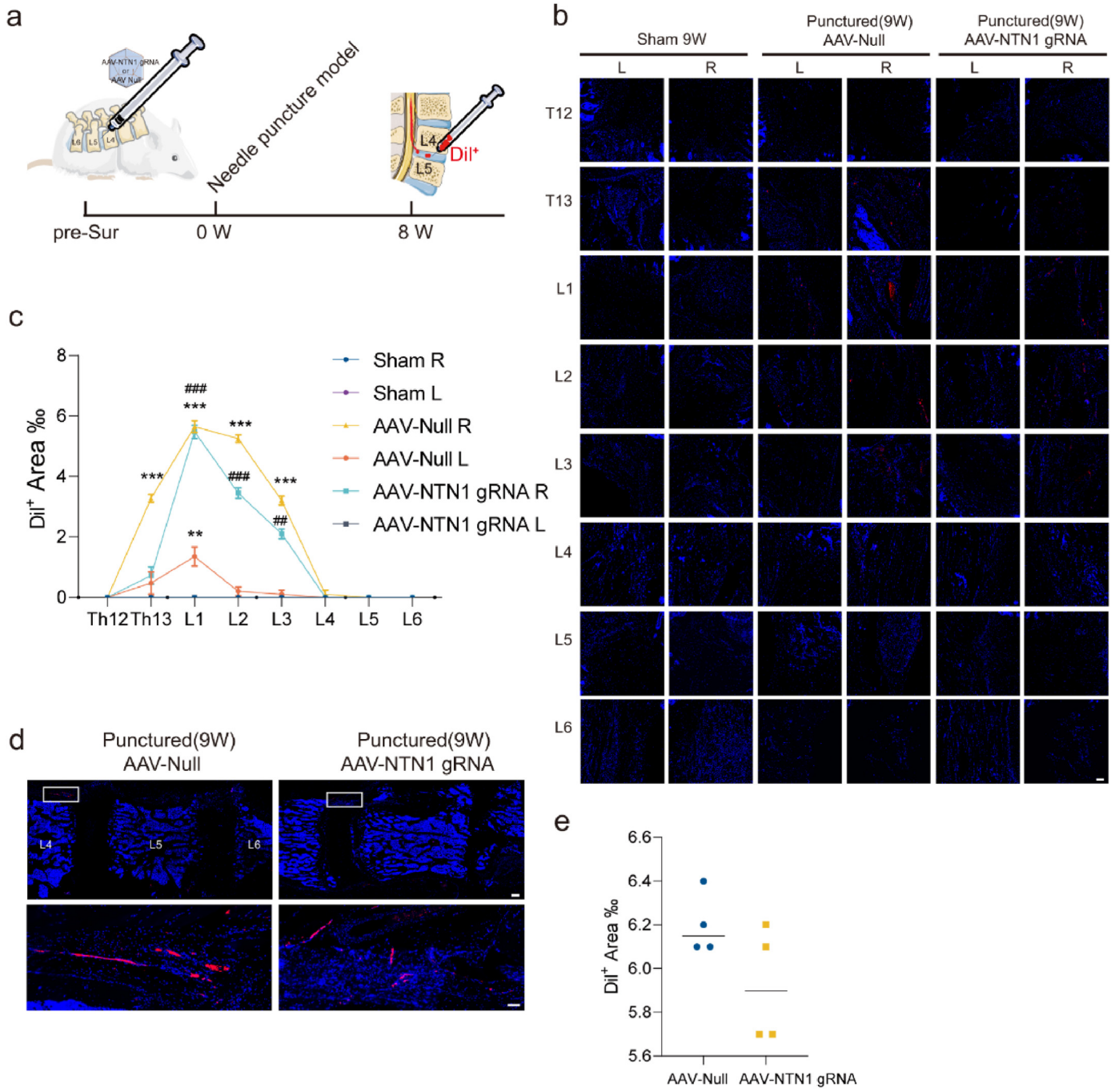

Figure 5. Nerve innervation in L4/5 IVD traced by retrograde and anterograde marker. a A graph of experiment pattern. Rats were inject with AAV-Null or AAV-NTN1 gRNA at L4/5 pre-surgery, and 1 week after that needle-punctured operation was performed through right-sided approach using 21G needle. Dil was injected into L4/5 IVD at 8 weeks after surgery. **b** Representative images of Dil$^+$ (red) neurons and DAPI (blue) nuclei staining at both sides of T12 - L6. Scale bar, 80 μm **c** Quantification of the Dil $^+$ area, **p < 0.01, ***p < 0.001 compared with sham group, #p < 0.05, ##p < 0.01 ###p < 0.001 compared with AAV-Null group at the corresponding segements (n = 4, each group). Results were means ± SD. **d** Representative images of Dil $^+$ area at L4/L5 IVD and **e** quantification of the Dil $^+$ area, after injected Dil in the right L1/2 DRGs at 8weeks. Scale bar, 500 μm (upper panel), 80 μm (lower panel). (For interpretation of the references to colour in this figure legend, the reader is referred to the Web version of this article.)

needle puncture surgery. We detected widespread Dil-labeled nerve fibers in the right side of L4/5 IVD in AVV-Null group, whereas just a little less in AAV-NTN1 gRNA group (Fig. 5d and e). In summary, these results show sensory innervation in L4/L5 degenerative IVDs mostly derived from L1 and L2 DRGs.

3.6. Transcription factor TCF3 negatively regulates Netrin-1 transcription

With a demonstration of the impact of nerve innervation and blood vessels ingrowth, we further explored the mechanism of up-regulation of Netrin-1 expression in degenerative NP cells. We used the JASPAR database (http://jaspar.genereg.net) and hTFtarget database

(http://bioinfo.life.hust.edu.cn/hTFtarget#!/) to predict potential transcriptional regulators of Netrin-1 and took the intersection of predicted transcription factors (TFs). The predict TFs were shown in Fig. S3A via volcano plot of IL-1β set. We purchased top 3 predict TFs overexpression plasmids according to – log (p value) in ascending order, and the predict score was shown in Fig. S3B. After overexpression of these TFs (Supplementary Fig. 3c and d), we found overexpression of TCF3 significantly decreased Netrin-1 mRNA expression and protein level (Fig. 6a–c) and with little effect on anabolism and catabolism of NP cells (Supplementary Fig. 3e).

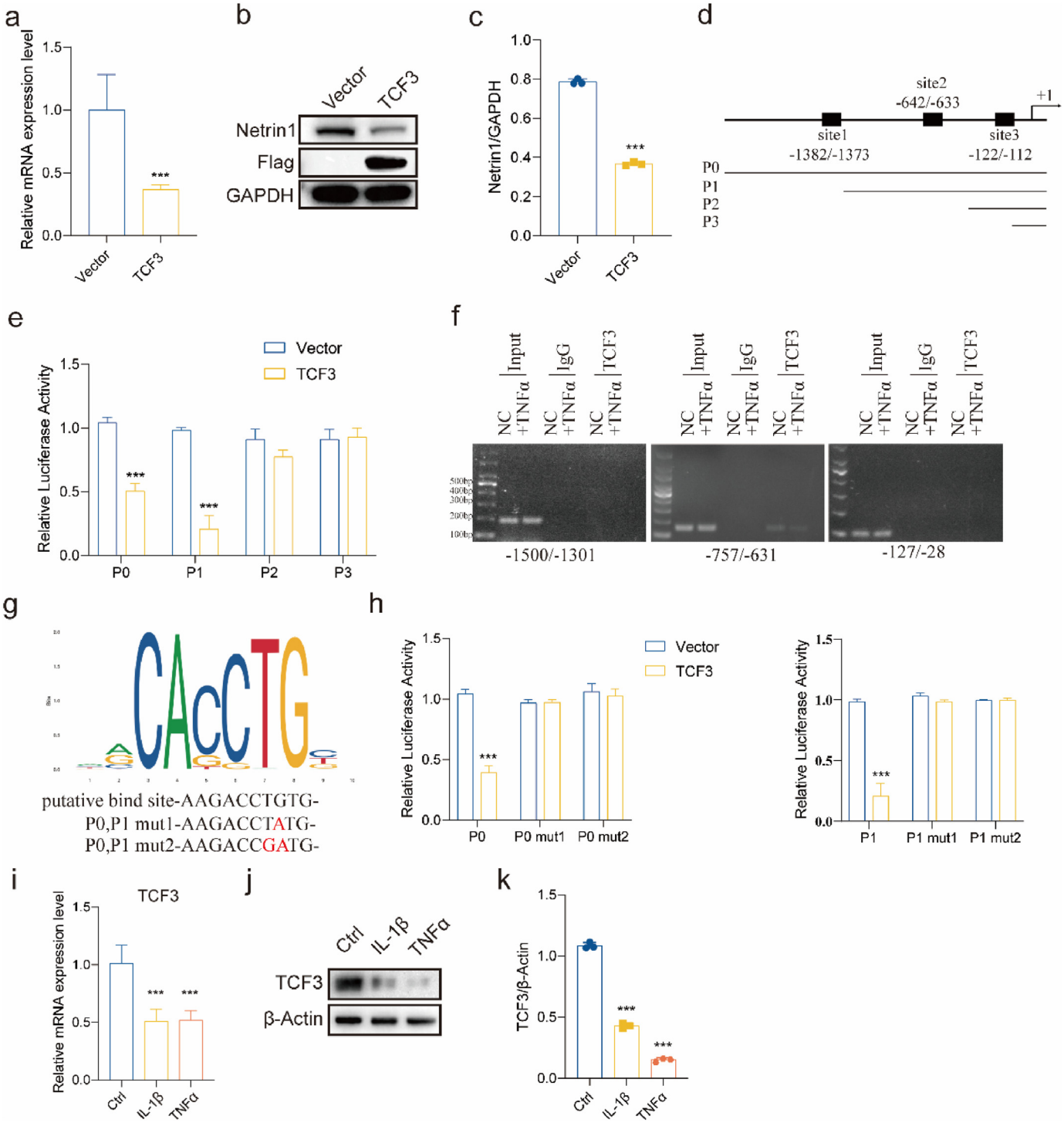

Figure 6. TCF3 negatively regulates Netrin-1 transcription. a Relative mRNA expression level of Netrin-1 in nucleus pulposus cells transfected with or without TCF3 overexpression (n = 6). **b** Protein expression of Netrin-1 transfected with or without TCF3 overexpression and **c** quantification of the blot (n = 3). **d** Putative TCF3-binding sites within the 2200 bp region of Netrin-1 promoter. **e** Netrin-1 promoter activity was assessed using luciferase assay in HEK-293 cells of P0, P1, P2, P3 and P4 segment (n = 3). **f** TCF3-binding sites of Netrin-1 promoter was detected by ChIP assay. **g** Mutation in the putative TCF3-binding site of the P0 and P1 segment. **h** P0 (left), P1 (right) and its mutant activity was analyzed by luciferase assay in HEK-293 cells (n = 3). **i** The mRNA level of TCF3 in nucleus pulposus cells treated with IL-1β or TNFα (n = 6). **j** Protein expression of TCF3 in nucleus pulposus cells treated with IL-1β or TNFα and **k** quantification of the blot (n = 3). ***p < 0.001 compared ctrl group. All data were shown as means ± SD.

Furthermore, according to the JASPAR database, the promoter region of Netrin-1 had 3 putative binding sites (Supplementary Fig. 3f). We created 4 sequences based on the Netrin-1 promoter segment, each of which had a different motif of potential transcriptional binding site (Fig. 6d). As illustrated in Fig. 6e, TCF3 stimulated negative luciferase activity in P0 and P1, indicating that sequence P1 is the active promoter segment. To further verify the binding motif, we then conducted a ChIP assay. While the segment of −1500 to −1301 bp and −127 to −28 bp exhibited no noticeable increase, the site of −757 to −631 bp showed obvious binding activity. Moreover, the increasing binding activity was alleviated while treated with TNFα (Fig. 6f). We further inserted mutations in the predicted binding site of promoter segments (P0, P1 mut1 and mut2) to validate the functional binding site and found that P0 and P1 mutant products abolished the negatively transcriptional regulation (Fig. 6g and h). In addition, we found TCF3 was reduced in NP cells after induced degeneration which was consistent with the findings in ChIP assay (Fig. 6i–k). Taken together, these findings revealed that degenerative NP cells mediated expression of Netrin-1 by TCF3, a negative transcription regulator of Netrin-1.

4. Discussion

The problem of LBP is tough to approach, because of the complexity of clinical symptoms [5]. It is commonly thought that inflammation, stress alteration or sympathetic efferent nerves may be blamed for some LBP problems, but the causes of LBP is still inconclusive [48,49]. The degenerative disc disease (DDD) is a major cause of LBP [50]. In this work, we found Netrin-1 played an important role in discogenic back pain via mediating sensory nerve fibers innervation and angiogenesis.

The sensory nerves distributed in the IVD are predominantly nociceptive, which forms the anatomical basis of discogenic back pain [51]. Nerves found within the IVDs in current study are primarily observed around fissures, which might give a path into the interior parts of the IVD where the fibrous matrix is disrupted [14]. However, the direct and exact factor of inducing the nerve invasion remains uncertain. Here we observed elevated expression of Netrin-1 in both cellular and tissue level, which is a specific cue functioned as axon guidance in mammalian nervous system. We found neuronal growth was promoted when treated with supernatants of degenerative NP cells, but this effect was suppressed when Netrin1 was knockdown. Further, nerve innervation in degenerative IVDs also decreased in needle-punctured rat model in the absence of Netrin-1. Additionally, Netrin-1 is also regarded to be a angiogenic factor which stimulates endothelial cell migration and proliferation in low concentration and becomes anti-angiogenic agent in high concentration [52,53]. In this study, we demonstrated that Netrin-1 expressed by degenerative NP cells exhibited strong inducing effect on vascular endothelial cells migration *in vitro* and controlled the growth direction of blood vessels *in vivo*. Moreover, we detected the upstream activation mechanism of Netrin-1. TCF3 is a pluripotency factor as a transcriptional repressor [54] which was found decrease during disc degeneration in our study. According to previous studies, β-catenin protein is upregulated in disc tissue samples from patients with disc degeneration [55,56]. Meanwhile, β-catenin could directly downregulate TCF3 expression in regulating pluripotency of stem cells [54,57] (GO: 2000036), which could explain the decrease of TCF3 in severe degenerated IVD. Particularly, our results show that TCF3 could suppress the expression of Netrin-1. Our data above suggest that in healthy IVD, Netrin-1 expression maintains a low level while TCF3 is highly expressed, and during disc degeneration, TCF3 expression decreases, which in turn abolished the down-regulation of Netrin-1. Then, Netrin-1 promotes both nerve and blood vessel ingrowth. The neovascularization provides trophic support for nerve growth, and in the process of DDD, the inflammation produces an amplification response, which causes peripheral nerve sensitization [58,59], leading to spinal pain eventually.

Our findings above shows that the immune-positive neural cells were found most in junctional regions of endplate and NP in moderate degenerative discs and found into NP area in sever degenerative discs. We suggest one reason for this is that endplate area exists osteoclasts that secret Netrin-1 [33]. The other reason is that NP is an enclosed tissue located in the center of the IVD, and largely rely on capillary diffusion through cartilage endplates for nutrient supply and metabolic waste transport [60,61]. NP cells secret Netrin-1 and transport it to endplate when IVD is mild or moderate degenerative which induces nerve growing towards junctional regions of endplate and NP. And in sever degenerative discs, there is annulus fibrosus fissures, allowing Netrin-1 expressed by NP cells to expose to the external environment, which induces nerve growing into NP area.

The dorsal section of L5 - S1 is innervated by the DRGs from L2 by the paraspinal branch, while L3 - L5 DRGs innervate through the sinuvertebral neuron, resulting in these LBP non-specific [62,63]. Here we used anterograde and retrograde nerve tracing models to identify the innervation pattern of lumber IVD, and found that nerve innervation in L4/5 discs was mostly derived from ipsilateral L1 and L2 DRGs.

Nonetheless, there were several issues in this work not in line with previous studies. The current theory for nerve and blood vessel ingrowth into the IVD is that NGF-expressing endothelial cells enter the IVD first, followed by sensory nerve fibers [64]. We did not find this to be the case in this investigation. We found that blood vessels did not invade deep into IVD as nerve fibers, which is consistent with Binch A.L.A et al. research [65]. We propose that the degree of degeneration may to blame.

Recent study believed Netrin-1 was expressed by macrophage or osteoclast in articular cartilage or cartilage endplate [13,33], but here we demonstrated NP cells could up-regulate Netrin-1 expression itself in degenerative IVD. Since previous study revealed that a subset of resident NP can eventually take on macrophage-like conversion [12,66,67], our findings suggest NP cells might exhibit potential macrophage phenotypes during degeneration.

In conclusion, we explicate that Netrin-1 leads to discogenic back pain via mediating nerve innervation and angiogenesis during IVD degeneration. Knockdown Netrin-1 by CRISPR/Cas9 or overexpressing TCF3 could impede this attractive effect and then relives the spinal allodynia. Therefore, we may safely draw a conclusion that Netrin-1 has the potential to be a promising treatment target of discogenic back pain in future.

Funding statement

This study was partially supported by Zhejiang Medical and Health Science and Technology project (No. 2021433841), Special Financial Grant from the China Postdoctoral Science Foundation (No. 2021TQ0279), Natural Science Foundation of Ningbo (No. 2019A610241). Zhejiang Provincial Natural Science Foundation of China under Grant (No. LQ20H170002, No. LGF19H180016).

Declaration of competing interest

The authors declare that they have no known competing financial interests or personal relationships that could have appeared to influence the work reported in this paper.

Acknowledgements

The institutional review board and ethics committee of Sir Run Shaw Hospital, Zhejiang University School of Medicine, examined and approved the study.

Appendix A. Supplementary data

Supplementary data to this article can be found online at https://doi.org/10.1016/j.jot.2022.11.006.

References

[1] Hoy D, Brooks P, Blyth F, Buchbinder R. The Epidemiology of low back pain. Best Pract Res Clin Rheumatol 2010;24:769–81.
[2] Hoy D, March L, Brooks P, Blyth F, Woolf A, Bain C, et al. The global burden of low back pain: estimates from the Global Burden of Disease 2010 study. Ann Rheum Dis 2014;73:968–74.
[3] Katz JN. Lumbar disc disorders and low-back pain: socioeconomic factors and consequences. J Bone Joint Surg Am 2006;88(Suppl 2):21–4.
[4] Deyo RA, Weinstein JN. Low back pain. N Engl J Med 2001;344:363–70.
[5] Urits I, Burshtein A, Sharma M, Testa L, Gold PA, Orhurhu V, et al. Low Back Pain, a Comprehensive Review: Pathophysiology, Diagnosis, and Treatment. Curr Pain Headache Rep 2019;23:23.
[6] Peng B-G. Pathophysiology, diagnosis, and treatment of discogenic low back pain. World J Orthop 2013;4:42–52.
[7] Freemont A, Peacock T, Goupille P, Hoyland J, O'Brien J, Jayson M. Nerve ingrowth into diseased intervertebral disc in chronic back pain. The Lancet 1997;350:178–81.
[8] Aoki Y, Ohtori S, Takahashi K, Ino H, Takahashi Y, Chiba T, et al. Innervation of the lumbar intervertebral disc by nerve growth factor-dependent neurons related to inflammatory pain. Spine 2004;29:1077–81.
[9] Aoki Y, Ohtori S, Takahashi K, Ino H, Douya H, Ozawa T, et al. Expression and co-expression of VR1, CGRP, and IB4-binding glycoprotein in dorsal root ganglion neurons in rats: differences between the disc afferents and the cutaneous afferents. Spine 2005;30:1496–500.
[10] Ohtori S, Takahashi K, Chiba T, Yamagata M, Sameda H, Moriya H. Substance P and calcitonin gene-related peptide immunoreactive sensory DRG neurons innervating the lumbar intervertebral discs in rats. Ann Anat Anat Anz Off Organ Anat Ges 2002;184:235–40.
[11] Ashton IK, Roberts S, Jaffray DC, Polak JM, Eisenstein SM. Neuropeptides in the human intervertebral disc. J Orthop Res Off Publ Orthop Res Soc 1994;12:186–92.
[12] Nerlich AG, Weiler C, Zipperer J, Narozny M, Boos N. Immunolocalization of phagocytic cells in normal and degenerated intervertebral discs. Spine 2002;27:2484–90.
[13] Zhu S, Zhu J, Zhen G, Hu Y, An S, Li Y, et al. Subchondral bone osteoclasts induce sensory innervation and osteoarthritis pain. J Clin Invest 2019;129:1076–93.
[14] Freemont AJ, Watkins A, Le Maitre C, Baird P, Jeziorska M, Knight MTN, et al. Nerve growth factor expression and innervation of the painful intervertebral disc. J Pathol 2002;197:286–92.
[15] Brown MF, Hukkanen MV, McCarthy ID, Redfern DR, Batten JJ, Crock HV, et al. Sensory and sympathetic innervation of the vertebral endplate in patients with degenerative disc disease. J Bone Joint Surg Br 1997;79:147–53.
[16] Burke JG, Watson RWG, McCormack D, Dowling FE, Walsh MG, Fitzpatrick JM. Intervertebral discs which cause low back pain secrete high levels of proinflammatory mediators. J Bone Joint Surg Br 2002;84:196–201.
[17] Burke JG, Watson RWG, Conhyea D, McCormack D, Dowling FE, Walsh MG, et al. Human nucleus pulposis can respond to a pro-inflammatory stimulus. Spine 2003;28:2685–93.
[18] Shamji MF, Setton LA, Jarvis W, So S, Chen J, Jing L, et al. Proinflammatory cytokine expression profile in degenerated and herniated human intervertebral disc tissues. Arthritis Rheum 2010;62:1974–82.
[19] Le Maitre CL, Richardson SMA, Baird P, Freemont AJ, Hoyland JA. Expression of receptors for putative anabolic growth factors in human intervertebral disc: implications for repair and regeneration of the disc. J Pathol 2005;207:445–52.
[20] Kitano T, Zerwekh JE, Usui Y, Edwards ML, Flicker PL, Mooney V. Biochemical changes associated with the symptomatic human intervertebral disk. Clin Orthop 1993:372–7.
[21] Oprée A, Kress M. Involvement of the proinflammatory cytokines tumor necrosis factor-alpha, IL-1 beta, and IL-6 but not IL-8 in the development of heat hyperalgesia: effects on heat-evoked calcitonin gene-related peptide release from rat skin. J Neurosci Off J Soc Neurosci 2000;20:6289–93.
[22] Obreja O, Schmelz M, Poole S, Kress M. Interleukin-6 in combination with its soluble IL-6 receptor sensitises rat skin nociceptors to heat, in vivo. Pain 2002;96:57–62.
[23] Obreja O, Biasio W, Andratsch M, Lips KS, Rathee PK, Ludwig A, et al. Fast modulation of heat-activated ionic current by proinflammatory interleukin 6 in rat sensory neurons. Brain J Neurol 2005;128:1634–41.
[24] Oka Y, Ibuki T, Matsumura K, Namba M, Yamazaki Y, Poole S, et al. Interleukin-6 is a candidate molecule that transmits inflammatory information to the CNS. Neuroscience 2007;145:530–8.
[25] Andratsch M, Mair N, Constantin CE, Scherbakov N, Benetti C, Quarta S, et al. A key role for gp130 expressed on peripheral sensory nerves in pathological pain. J Neurosci Off J Soc Neurosci 2009;29:13473–83.
[26] Barendse GA M, van den Berg SGM, Kessels AHF, Weber WEJ, van Kleef M. Randomized Controlled Trial of Percutaneous Intradiscal Radiofrequency Thermocoagulation for Chronic Discogenic Back Pain: Lack of Effect From a 90-Second 70 C Lesion. Spine 2001;26:287–92.
[27] Kapural L, Hayek S, Malak O, Arrigain S, Mekhail N. Intradiscal Thermal Annuloplasty Versus Intradiscal Radiofrequency Ablation for the Treatment of Discogenic Pain: A Prospective Matched Control Trial. Pain Med 2005;6:425–31.
[28] Ding Q, Liao S-J, Yu J. Axon guidance factor netrin-1 and its receptors regulate angiogenesis after cerebral ischemia. Neurosci Bull 2014;30:683–91.
[29] Durrani S, Haider KH, Ahmed RPH, Jiang S, Ashraf M. Cytoprotective and Proangiogenic Activity of Ex-Vivo Netrin-1 Transgene Overexpression Protects the Heart Against Ischemia/Reperfusion Injury. Stem Cells Dev 2012;21:1769–78.
[30] Bradford D, Cole SJ, Cooper HM. Netrin-1: diversity in development. Int J Biochem Cell Biol 2009;41:487–93.
[31] Xu K, Wu Z, Renier N, Antipenko A, Tzvetkova-Robev D, Xu Y, et al. Structures of netrin-1 bound to two receptors provide insight into its axon guidance mechanism. Science 2014;344:1275–9.
[32] Dun X-P, Parkinson DB. Classic axon guidance molecules control correct nerve bridge tissue formation and precise axon regeneration. Neural Regen Res 2020;15:6–9.
[33] Ni S, Ling Z, Wang X, Cao Y, Wu T, Deng R, et al. Sensory innervation in porous endplates by Netrin-1 from osteoclasts mediates PGE2-induced spinal hypersensitivity in mice. Nat Commun 2019;10:5643.
[34] Wilson BD, Ii M, Park KW, Suli A, Sorensen LK, Larrieu-Lahargue F, et al. Netrins promote developmental and therapeutic angiogenesis. Science 2006;313:640–4.
[35] Wang Y, Che M, Xin J, Zheng Z, Li J, Zhang S. The role of IL-1β and TNF-α in intervertebral disc degeneration. Biomed Pharmacother 2020;131:110660.
[36] Francisco V, Pino J, González-Gay MÁ, Lago F, Karppinen J, Tervonen O, et al. A new immunometabolic perspective of intervertebral disc degeneration. Nat Rev Rheumatol 2022;18:47–60.
[37] Keorochana G, Johnson JS, Taghavi CE, Liao J-C, Lee K-B, Yoo JH, et al. The effect of needle size inducing degeneration in the rat caudal disc: evaluation using radiograph, magnetic resonance imaging, histology, and immunohistochemistry. Spine J 2010;10:1014–23.
[38] Glaeser JD, Tawackoli W, Ju DG, Yang JH, Kanim LE, Salehi K, et al. Optimization of a rat lumbar IVD degeneration model for low back pain. JOR Spine 2020;3:e1092.
[39] Hua J, Shen N, Wang J, Tao Y, Li F, Chen Q, et al. Small Molecule-Based Strategy Promotes Nucleus Pulposus Specific Differentiation of Adipose-Derived Mesenchymal Stem Cells. Mol Cells 2019;42:661–71.
[40] Singh K, Masuda K, An HS. Animal models for human disc degeneration. Spine J 2005;5:S267–79.
[41] Chaplan SR, Bach FW, Pogrel JW, Chung JM, Yaksh TL. Quantitative assessment of tactile allodynia in the rat paw. J Neurosci Methods 1994;53:55–63.
[42] Bonin RP, Bories C, De Koninck Y. A Simplified Up-Down Method (SUDO) for Measuring Mechanical Nociception in Rodents Using von Frey Filaments. Mol Pain 2014;10. 1744-8069-10-26.
[43] Mills C, LeBlond D, Joshi S, Zhu C, Hsieh G, Jacobson P, et al. Estimating Efficacy and Drug ED50's Using von Frey Thresholds: Impact of Weber's Law and Log Transformation. J Pain 2012;13:519–23.
[44] Brennan TJ, Vandermeulen EP, Gebhart GF. Characterization of a rat model of incisional pain. PAIN 1996;64:493–502.
[45] Taylor AM, Blurton-Jones M, Rhee SW, Cribbs DH, Cotman CW, Jeon NL. A microfluidic culture platform for CNS axonal injury, regeneration and transport. Nat Methods 2005;2:599–605.
[46] Lama P, Le Maitre CL, Harding IJ, Dolan P, Adams MA. Nerves and blood vessels in degenerated intervertebral discs are confined to physically disrupted tissue. J Anat 2018;233:86–97.
[47] Zhang S, Hu B, Liu W, Wang P, Lv X, Chen S, et al. The role of structure and function changes of sensory nervous system in intervertebral disc-related low back pain. Osteoarthritis Cartilage 2021;29:17–27.
[48] Nakamura SI, Takahashi K, Takahashi Y, Yamagata M, Moriya H. The afferent pathways of discogenic low-back pain. Evaluation of L2 spinal nerve infiltration. J Bone Joint Surg Br 1996;78:606–12.
[49] Ohtori S, Miyagi M, Inoue G. Sensory nerve ingrowth, cytokines, and instability of discogenic low back pain: A review. Spine Surg Relat Res 2018;2:11–7.
[50] Andersson GB. Epidemiological features of chronic low-back pain. Lancet Lond Engl 1999;354:581–5.
[51] Groh AMR, Fournier DE, Battié MC, Séguin CA. Innervation of the Human Intervertebral Disc: A Scoping Review. Pain Med Malden Mass 2021;22:1281–304.
[52] Layne K, Ferro A, Passacquale G. Netrin-1 as a novel therapeutic target in cardiovascular disease: to activate or inhibit? Cardiovasc Res 2015;107:410–9.
[53] Park KW, Crouse D, Lee M, Karnik SK, Sorensen LK, Murphy KJ, et al. The axonal attractant Netrin-1 is an angiogenic factor. Proc Natl Acad Sci USA 2004;101:16210–5.
[54] Wray J, Kalkan T, Gomez-Lopez S, Eckardt D, Cook A, Kemler R, et al. Inhibition of glycogen synthase kinase-3 alleviates Tcf3 repression of the pluripotency network and increases embryonic stem cell resistance to differentiation. Nat Cell Biol 2011;13:838–45.
[55] Wang M, Tang D, Shu B, Wang B, Jin H, Hao S, et al. Conditional activation of β-catenin signaling in mice leads to severe defects in intervertebral disc tissue. Arthritis Rheum 2012;64:2611–23.
[56] Smolders LA, Meij BP, Riemers FM, Licht R, Wubbolts R, Heuvel D, et al. Canonical Wnt signaling in the notochordal cell is upregulated in early intervertebral disk degeneration. J Orthop Res Off Publ Orthop Res Soc 2012;30:950–7.
[57] Fan R, Kim YS, Wu J, Chen R, Zeuschner D, Mildner K, et al. Wnt/Beta-catenin/Esrrb signalling controls the tissue-scale reorganization and maintenance of the pluripotent lineage during murine embryonic diapause. Nat Commun 2020;11:5499.
[58] Wuertz K, Haglund L. Inflammatory mediators in intervertebral disk degeneration and discogenic pain. Glob Spine J 2013;3:175–84.
[59] Richards J, Tang S, Gunsch G, Sul P, Wiet M, Flanigan DC, et al. Mast Cell/Proteinase Activated Receptor 2 (PAR2) Mediated Interactions in the Pathogenesis of Discogenic Back Pain. Front Cell Neurosci 2019;13:294.
[60] Guiot BH, Fessler RG. Molecular Biology of Degenerative Disc Disease. Neurosurgery 2000;47:1034–40.
[61] Urban JPG, Smith S, Fairbank JCT. Nutrition of the Intervertebral Disc. Spine 2004;29:2700–9.

[62] Aoki Y, Takahashi Y, Takahashi K, Chiba T, Kurokawa M, Ozawa T, et al. Sensory innervation of the lateral portion of the lumbar intervertebral disc in rats. Spine J 2004;4:275–80.
[63] Takahashi Y, Chiba T, Kurokawa M, Aoki Y, Takahashi K, Yamagata M. Stereoscopic Structure of Sensory Nerve Fibers in the Lumbar Spine and Related Tissues. Spine 2003;28:871–80.
[64] Bailey JF, Liebenberg E, Degmetich S, Lotz JC. Innervation patterns of PGP 9.5-positive nerve fibers within the human lumbar vertebra. J Anat 2011;218:263–70.
[65] Binch ALA, Cole AA, Breakwell LM, Michael ALR, Chiverton N, Creemers LB, et al. Nerves are more abundant than blood vessels in the degenerate human intervertebral disc. Arthritis Res Ther 2015;17:370.
[66] Nakazawa KR, Walter BA, Laudier DM, Krishnamoorthy D, Mosley GE, Spiller KL, et al. Accumulation and localization of macrophage phenotypes with human intervertebral disc degeneration. Spine J Off J North Am Spine Soc 2018;18:343–56.
[67] Yamamoto Y, Kokubo Y, Nakajima H, Honjoh K, Watanabe S, Matsumine A. Distribution and Polarization of Hematogenous Macrophages Associated with the Progression of Intervertebral Disc Degeneration. Spine 2022;47:E149–58.